# Receiver-Level Robustness Concepts for EGNSS Timing Services

Martti Kirkko-Jaakkola, Sarang Thombre, Salomon Honkala, Stefan Söderholm, Sanna Kaasalainen, and Heidi Kuusniemi, *Finnish Geospatial Research Institute, Kirkkonummi, Finland*

Hein Zelle and Henk Veerman, *Netherlands Aerospace Centre, Marknesse, The Netherlands*

Anders Wallin, *VTT MIKES Metrology, Espoo, Finland*

Kjell Arne Aarmo and Juan Pablo Boyero, *European Commission, Brussels, Belgium*

**BIOGRAPHIES**

**Martti Kirkko-Jaakkola** received his M.Sc. and D.Sc. (Tech.) degrees from Tampere University of Technology, Finland, in 2008 and 2013, respectively. From 2006 till 2013 he worked with the Department of Pervasive Computing, Tampere University of Technology, including research visits to the Technical University of Munich, Germany, and the European Space Research and Technology Centre, The Netherlands. Currently, he works as a Research Manager at the Finnish Geospatial Research Institute (FGI) in Kirkkonummi, Finland; his research interests include low-cost precise satellite positioning, microelectromechanical inertial sensors, and GNSS-based time transfer.

**Sarang Thombre** is a Research Manager and deputy leader of the Satellite and Radio Navigation research group at the Department of Navigation and Positioning of FGI. He earned his D. Sc. (Tech) degree in April 2014 from Tampere University of Technology, Finland. He is an External Project Reviewer for the European GNSS Agency within the Horizon 2020 Galileo programme, and a member of the Board of the Nordic Institute of Navigation. His research interests are in multi-GNSS, multi-frequency, and Timing receiver implementation and performance validation, interference detection, and maritime situational awareness.

**Salomon Honkala** is a researcher at the Department of Navigation and Positioning at FGI. He received his M.Sc. degree from the School of Electrical Engineering, Aalto University, Finland, in 2016.

**Stefan Söderholm** is the leader of the Satellite and Radio Navigation research group at the Department of Navigation and Positioning at FGI, Finland, since 2013. From 2004 he headed the Fastrax software development team, and 2008 he became Vice-President of R&D at Fastrax Ltd. Söderholm has also worked as a Project Manager in the algorithm and signal processing team at u-blox Ltd. He received his M.Sc. degree from Åbo Akademi University and his Licentiate degree from University of Turku, Finland.

**Sanna Kaasalainen** is a Research Professor at the Department of Navigation and Positioning at the Finnish Geospatial Research Institute (FGI) and a docent (Adjunct Professor) in laser measurement physics at Aalto University School of Engineering. She received a PhD degree in astronomy from the University of Helsinki in 2003.

**Heidi Kuusniemi** is a Professor and Director of the Department of Navigation and Positioning at the Finnish Geospatial Research Institute (FGI) and a docent (Adjunct Professor) at Aalto University and Tampere University of Technology, Finland. She received her doctoral degree from Tampere University of Technology (TUT), Finland, in 2005. Part of her doctoral research was conducted in the PLAN group of the Department of Geomatics Engineering at the University of Calgary, Canada. From January to March 2017 she was a visiting scholar at the GPS laboratory of Stanford University.

**Hein Zelle** is a GNSS R&D engineer at the Netherlands Aerospace Centre (NLR). He has a MSc degree in Technical Physics, and received his PhD in Physical Oceanography in 2004, based on a study of El Nino southern oscillation, performed at KNMI in the Netherlands. In 2014 he joined NLR, starting research activities in the field of GNSS. His has worked on correction of atmospheric delays, measuring high accuracy ionospheric parameters based on combining radio-astronomical observations

Paper first presented at the ION GNSS+ conference, Portland, Oregon, September 2017.

with GNSS observables, and improving tropospheric error correction models for aviation. He currently focuses on GNSS-based timing and GNSS interference.

**Henk Veerman** received his MSc degree in Experimental Physics from the University of Amsterdam in 1984. Now as a senior scientist at NLR, he works on novel technologies for application in aeronautics, with a focus on GNSS-based navigation. He has been involved in GNSS research since 2000, investigating EGNOS and Galileo performances and prospects for aeronautical application, studies on GNSS integrity, GNSS signal atmospheric propagation, RF interference, he is working on Multi Constellation / Multi Frequency GBAS concepts for Cat II / III approach and landing and GNSS-based timing.

**Anders Wallin** is a Senior Scientist at VTT MIKES Metrology. He received his PhD from the University of Helsinki in 2011. Since 2012 he has worked in the Time & Frequency metrology field and his research interests include microwave and optical atomic clocks, time transfer techniques, and metrological instrumentation.

**Kjell Arne Aarmo** is since 2015 working at the EC in the definition of the evolution of the Galileo and EGNOS missions. He is on a temporary leave from his senior adviser position at the Norwegian Spacecentre. He received a M.Sc. by the Norwegian university of science and technology in 1995.

**Juan Pablo Boyero** is since 2012 working at the EC in the definition of the evolution of the Galileo and EGNOS missions. Before he worked within the Galileo System Performance area and acting both as System Prime as well as Technical Support to System Prime. He received a M.Sc. by the Escuela Técnica Superior de Ingenieros de Telecomunicación of the Universidad Politécnica de Madrid. He has passed the course on Safety Critical Systems by the University of Oxford, UK.


## ABSTRACT

GNSS-based time transfer is utilized in various critical infrastructures as it provides important advantages which are being increasingly exploited. In this paper, we present the various implementation options for robust timing service concepts based on European GNSS (EGNSS), i.e., Galileo and EGNOS, that are expected to further foster the use of EGNSS timing; this concept can make use of the redundancy of measurements and of available GNSS constellations. The stability properties of the local oscillator, which are known to the designer, are also exploited. The algorithms are developed to account for cases where several measurement faults occur simultaneously, which is a possible scenario in land-based reception conditions. Furthermore, we derive time protection level equations to quantify the integrity of the GNSS time solution as a function of the false alarm and missed detection probabilities as well as the maximum number of simultaneous outliers to be accounted for. Some of the considered fault scenarios can only be detected but not rectified by the algorithms: in such case, holdover, i.e. processing based on the local oscillator alone, is triggered. Thus, the performance in these scenarios is dependent on the stability of the local oscillator; in this paper, the analysis is based on a low-cost temperature-compensated crystal oscillator. The effect of the robustness concepts is illustrated with a set of experiments which show that when implemented in a timing GNSS receiver, the algorithms presented can deal with failures that affect individual satellites or even an entire constellation. Local disturbances affecting the receiver can also be effectively detected. Specifying EGNSS timing as proper services along with well-defined procedures for testing receiver compliance paves the road for standardizing and certifying robust EGNSS timing receivers, which would be beneficial for many applications and in particular in safety or liability critical use cases.


## INTRODUCTION

The inherent time determination capability of GNSS positioning services is used in various applications as it offers a cost-effective time reference that is traceable to a Coordinated Universal Time (UTC) realization, i.e. to a UTC(*k*) time scale (Lombardi 2006; Bauch and Whibberley 2017). In fact, GNSS based timing plays an important role in various critical infrastructures in, e.g., the energy, financial, and telecommunications sectors. It is well known that GNSS measurements unfortunately are subject to a range of threats which can take place at signal transmission, propagation, or reception; a GNSS timing failure in critical applications can have severe consequences (Mujunen et al. 2016).

Timing is currently not offered as a well-defined, stand-alone service by any GNSS: for example, the timing performance commitments of GPS and Galileo are stated as part of the Standard Positioning Service and Open Service definitions, respectively. In other words, timing can currently be seen as a capability of positioning services. Given the importance of GNSS timing in critical infrastructure, specifying GNSS timing as a well-defined service could bring added value in two ways. First, the performance commitments should be defined in terms of Key Performance Indicators (KPIs) that are commonly used for stating the requirements of timing applications. Second, the service should specify a series of standardized tests which can be used to evaluate different processing strategies in a uniform way and with respect to standardized criteria. Reference receiver algorithms should also be developed and used as comparison term. This is, for example, the path undertaken for the development of the Advanced Receiver Autonomous Integrity Monitoring (ARAIM) service where a reference algorithm has been

developed. In this context, reference algorithms should yield the specified performance in a robust way. In order to achieve this, the European Commission has initiated the "Advanced Mission Concepts: R&D for Robust EGNSS Timing Services" project under the Horizon 2020 framework programme. The objective of the project is to define stand-alone timing services for European GNSS (EGNSS), i.e., Galileo and EGNOS.

Suitable KPIs for the timing services were identified in (Kirkko-Jaakkola et al. 2017). This paper proposes a set of implementation options that can serve as reference processing algorithms for the envisioned timing services. Time Receiver Autonomous Integrity Monitoring (T-RAIM) is a key concept for robust timing (Geier et al. 1995) and it is thus included in the proposed processing chain. In this respect, we derive the Time Protection Level (TPL) to quantify the obtained integrity level. Additional resilience is obtained by implementing interference detection and utilizing redundant GNSS constellations. Timing receivers can also use the Local Oscillator (LO) itself as a robustness measure; it resembles the concept of loose coupling of GNSS and Inertial Navigation Systems (INSs). The purpose of the envisioned timing services is not to improve the accuracy of EGNSS based timing but its reliability. Since timing accuracy is not the main driver for the services considered here, the use of carrier phase measurements is not addressed (Defraigne et al. 2008).

The remainder of this paper is organized as follows. First, the basics of EGNSS based timing as well as the most relevant threat scenarios are reviewed. Then, robustness algorithms to mitigate the threats at various stages of the processing chain are described. Finally, the effectiveness of the proposed concepts is analyzed in a set of experiments.

## OVERVIEW OF EGNSS BASED TIMING

In this paper, we assume three characteristics for a timing GNSS receiver. First, it has to be capable of outputting a Pulse Per Second (PPS) signal or a frequency output, implemented, for example, as a 10 MHz pure sinusoid. Second, the receiver has access to an oscillator with known stability properties; this can be the internal LO of the receiver or an external oscillator. This oscillator is steered based on GNSS measurements. When no GNSS updates are available, the oscillator can continue operation autonomously with gradually degrading performance; this mode of operation is called holdover. Third, the antenna is assumed to be fixed to precisely known coordinates.

In this section, the basics of EGNSS based time determination are reviewed. First, the service provision environment for the envisioned timing services is described. Then, the receiver-side signal processing involved is presented, followed by a description of the threat scenarios that were identified as the most relevant. Since the principles are similar for EGNOS and Galileo, the two systems are addressed together with differences pointed out where necessary.

### EGNSS Timing Service Provision Environment

The high-level architecture of EGNSS based timing is illustrated in Figure 1. The system time is generated at the control centre based on inputs from a set of atomic clocks. Each system has its own system time scale: EGNOS uses the EGNOS Network Time (ENT) whereas Galileo is based on the Galileo System Time (GST). In the case of EGNOS, the atomic clocks are located at the Ranging and Integrity Monitoring Stations (RIMS) and the control centre is known as the Central Processing Facility (CPF); for Galileo, the atomic clock inputs are obtained from the Precise Timing Facility (PTF) and processed at the Galileo Control Centre (GCC).

Traceability to a UTC($k$) time scale is ensured by inputs from a timing laboratory. ENT is traceable to UTC(OP) maintained by the Observatoire de Paris whereas Galileo provides conversion parameters to the UTC prediction maintained by the Galileo Time Service Provider (TSP). Note that this TSP does not correspond to the entity operating the envisioned robust timing services. Finally, the satellite clocks are synchronized to the system time scale and the necessary conversion parameters are uploaded, and this information is broadcast to the end users in form of the Signal-In-Space (SIS). The users retrieve the current time by processing the SIS as described in the following section.

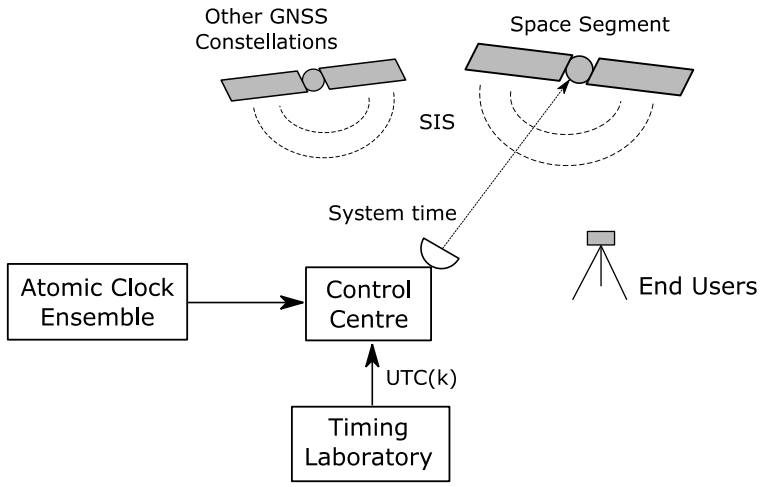


**Figure 1: High-level architecture of EGNSS based timing.**

Although this is currently limited to GPS only, other GNSS constellations play a role in both EGNOS and Galileo based timing. As an augmentation system, EGNOS provides corrections to GPS measurements; currently, geostationary ranging is not supported by EGNOS. Therefore, ENT is obtained by applying the EGNOS corrections to GPS measurements, which converts the reference time scale from GPS Time (GPST) to ENT. The offset between these two time scales is at the level of tens of nanoseconds because ENT is continuously steered towards GPST (European GNSS Agency 2015). Although Galileo measurements can be used alone to obtain the GST which is steered towards the UTC realization maintained by the TSP, they can be used jointly with GPS using the conversion parameters to GPST that is provided in the form of the Galileo/GPS Time Offset (GGTO). Note that although, according to the specifications, the GGTO provided is more accurate than the UTC conversion parameters (European Commission 2016a), one must also account for possible receiver and antenna dependent hardware biases between the observed GST and GPST (Hegarty et al. 2004).

**Basic Receiver-Side Processing Chain**

A schematic representation of receiver processing chain for EGNSS based time determination is shown in Figure 2. After capturing the radio frequency SIS, the task of the radio frontend is to convert it to digital samples at the baseband frequency, for which the LO provides the reference frequency signal. These samples are used to acquire and track the satellite signals, based on which pseudorange measurements are constructed and the navigation data are decoded. These measurements have to be compensated for systematic errors such as satellite clock biases and ionospheric delays; EGNOS users also apply the augmentation data at this point. The error-compensated measurements are then used for estimating the local clock offset with respect to the system time. If necessary, the obtained offset is converted to UTC using the parameters broadcast in the navigation data. Finally, the time solution is utilized to steer the LO to fine-tune the PPS and/or frequency reference output.

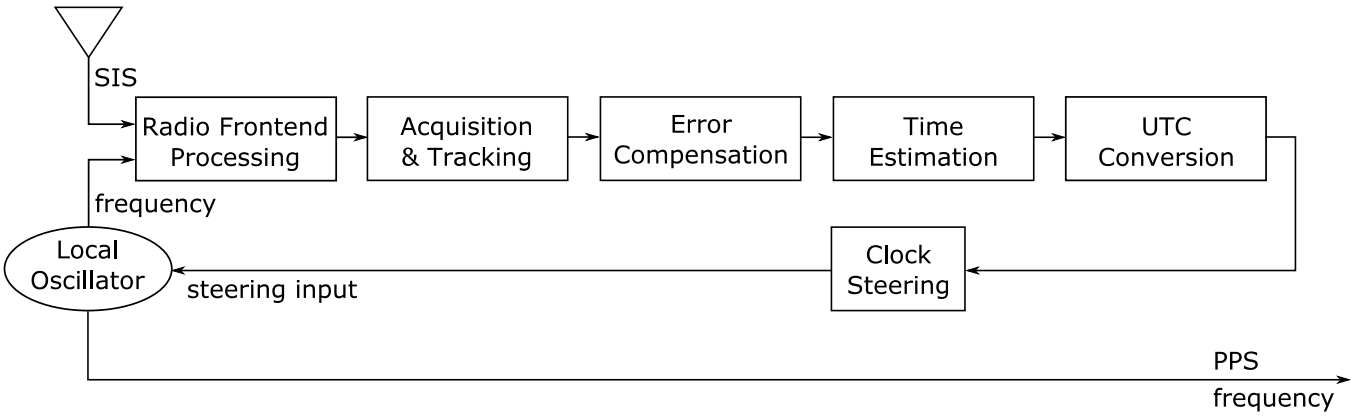


**Figure 2: Basic processing steps for EGNSS based timing.**

It is noteworthy that when the antenna coordinates are known, the problem of clock bias estimation reduces to a univariate linear system of equations for each system. A multi-constellation receiver can solve for the clock biases of each constellation separately as there are no common unknowns shared between systems.

For mitigating ionospheric delays, EGNOS timing service users shall use the grid ionosphere model included in the augmentation data. Galileo users, however, have two options: dual-frequency receivers are expected to form ionosphere-free observables using the E1 and E5 bands; single-frequency users need to use the NeQuick G model (European Commission 2016b) for ionospheric corrections. Note that dual-frequency users may occasionally have to resort to the NeQuick G model if one of the frequency bands is temporarily unavailable, e.g., because of radio frequency interference.

In the following sections, failure scenarios concerning this processing chain are described, and enhancements to address these threats are proposed.

### Threat Scenarios

In the context of the envisioned robust timing services, a threat is considered to be anything that prevents the GNSS receiver from determining the correct time in the time scale of interest, which can be the system time or UTC(*k*). When developing the robust timing services, the following three categories of threat scenarios were identified as the most relevant.

*Radio frequency interference, jamming, and spoofing*. Because of the low signal power, GNSS receivers are particularly susceptible to local radio frequency interference and even malicious jamming. Furthermore, spoofing attacks and their mitigation have gained a lot of research interest recently. It is noteworthy that even the most trivial form of spoofing, i.e., delayed repeating of received satellite signals, can have a significant impact on a timing receiver operating at a fixed location. This attack is known as meaconing or replay spoofing. Not only is meaconing rather easy to implement, but even encrypted signals can be repeated without knowing the decryption key.

*Individual satellite faults*. A subset of the GNSS measurements can be corrupted as a result of, e.g., faulty broadcast orbit parameters, erroneous clock correction parameters for individual satellites, or excessive ionospheric or multipath errors. These individual outliers result in a mutually inconsistent set of observations.

*Constellation-wide failure*. Errors in the ground segment, e.g., the use of an erroneous Earth orientation parameter realization in the prediction of satellite orbits, can cause all satellites of one system to start broadcasting biased ephemerides (Blanch et al. 2013). As opposed to the individual faults scenario, in this case the measurements are mutually consistent although all of them are lead to erroneous timing information. A possible cause of this threat is an error in the broadcast system time to UTC(*k*) conversion parameters which are common to all satellites in one constellation.

## TECHNICAL CONCEPTS FOR IMPROVED ROBUSTNESS

In this section, the methods for ensuring the robustness of the envisioned EGNSS timing services are described. The concepts are presented in the order of execution in the signal processing chain, the basic version of which was reviewed in the previous section. First, pre-screening of the data is addressed in order to detect the presence of interference. Then, measurement self-consistency verification for one constellation by means of T-RAIM is described, followed by the optional cross-check between constellation-level solutions. Finally, the known stability properties of the LO are used to further enhance the resilience of the system.

### Interference Detection

In the scope of the envisioned robust timing services, the goal is not to mitigate radio frequency attacks as such. Instead, the receiver is expected to detect them and enter holdover instead of using potentially compromised signals. It is possible to actually mitigate interfering radio signals, e.g., by using beam-forming antennas, but since such equipment tend to increase the hardware cost, they were not included in the specification of the developed robust timing services.

A plethora of algorithms for detecting the presence of interfering or jamming signals have been proposed in the literature (Borio et al. 2016). In general, these algorithms are based on monitoring either the automatic gain control (AGC) of the radio frontend, the distribution of the baseband samples after the analog-to-digital conversion, or the Carrier-to-Noise power spectral density ($C/N_0$) values estimated from the tracking loops. The approach of monitoring the AGC gain values (Bastide et al. 2003) was chosen to be part of the receiver-side processing specification for the envisioned timing services because it can work even when no satellites are tracked, yet being straightforward to implement as access to baseband samples is not needed. In the test results, we will also evaluate the feasibility of detecting a meaconing attack based on the AGC gain.

**T-RAIM**

Detecting the presence of individual measurement outliers is a vital part of GNSS quality control. The algorithm described in this paper is based on the method presented in (Geier et al. 1995). However, we relax the assumption of identically distributed measurements made by (Geier et al. 1995). Moreover, we derive the TPL to quantify the integrity.

The input to the time estimation and T-RAIM algorithms are a set of $N$ error-compensated pseudorange measurements $\rho_i$ and their estimated residual error standard deviations, $\sigma_i$, where $i = 1, \dots, N$. In order for the T-RAIM algorithm to be able to operate, we require as the minimum number of observations per each constellation $N \geq 2$. Given the known antenna coordinates, the best linear unbiased estimate of the receiver clock offset $\widehat{\delta t}$ with respect to the GNSS system time reduces to a weighted average:

$$\widehat{\delta t} = \frac{\sum_{i=1}^{N} \frac{\rho_i - r_i}{\sigma_i^2}}{c \sum_{i=1}^{N} \sigma_i^{-2}} \tag{1}$$

where $r_i$ denotes the known physical distance between the $i$th satellite and the receiver antenna, and $c$ is the speed of light. The error standard deviation of the clock offset estimate, $\widehat{\delta t}$, is obtained as

$$\hat{\sigma} = \sqrt{\frac{1}{c^2 \sum_{i=1}^{N} \sigma_i^{-2}}}. \tag{2}$$

The T-RAIM algorithm begins by testing if there are any faults present in the set of measurements or not; this step is commonly referred to as the global test. If no faults are present, the residuals $(\rho_i - r_i - c\widehat{\delta t})$ should follow a zero-mean normal distribution with standard deviation $\sigma_i$. This implies that the vector of residuals normalized by the respective standard deviations should have a squared Euclidian norm that follows the chi-square distribution with $(N - 1)$ degrees of freedom:

$$\sum_{i=1}^{N} \frac{\left(\rho_i - r_i - c\,\widehat{\delta t}\right)^2}{\left(\sigma_i^{UERE}\right)^2} \sim \chi^2(N-1). \tag{3}$$

Equation 3 allows the test of the no-fault hypothesis $H_0$ with a pre-defined false alarm probability, $p_{FA}$. If the value of the test statistic on the left-hand side falls below the critical value, the set of measurements is regarded as mutually consistent and the T-RAIM algorithm terminates. Otherwise, outliers need to be excluded one at a time until either the chi-square test is passed or less than half of the original set of measurements remain. In the RAIM literature, the exclusion process typically involves a set of local tests to identify the faulty measurements; however, with the linear univariate timing problem, we replace the local tests by directly excluding the measurement that has the largest normalized residual and continue the T-RAIM algorithm recursively. Note that this approach does not work well for the nonlinear model with unknown antenna coordinates where the residuals become highly correlated.

To derive the TPL, one must first note that if outliers are present, the residuals $(\rho_i - r_i - c\widehat{\delta t})$ no longer have zero-mean distributions. Consequently, the squared Euclidian norm of the normalized residuals has a noncentral chi-square distribution. First, we must determine the noncentrality parameter, $\delta$, that causes the global test to fail subject to a pre-defined probability of missed detection, $p_{MD}$, when the critical value is determined based on the given false alarm probability, $p_{FA}$. Then, the TPL is defined as the maximum possible impact on the time estimate, $\widehat{\delta t}$, caused by a set of outliers corresponding to the noncentrality parameter, $\delta$. This logic is similar to the derivation of protection levels for conventional positioning algorithms (Kuusniemi 2005). The relationship between $\delta$, $p_{FA}$, and $p_{MD}$ is illustrated in Figure 3. The cumulative density function (cdf) of the biased distribution with noncentrality parameter $\delta$ below the critical value equals the missed detection probability, $p_{MD}$. Simultaneously, the complementary cdf of the unbiased fault-free distribution beyond the critical value equals the false alarm rate, $p_{FA}$. With the two probabilities fixed, the value of $\delta$ that satisfies the equality can be determined using the respective inverse cumulative chi-square density functions.

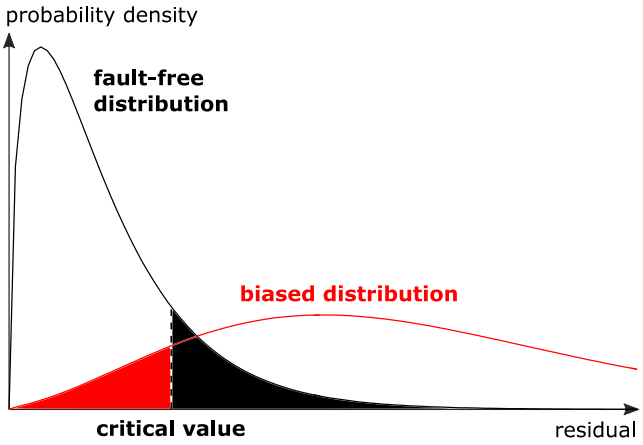


**Figure 3: Relationship between the noncentrality parameter, the false alarm and missed detection probabilities.**

Let assume that the measurements are sorted with ascending error standard deviations, i.e., $\sigma_1 \leq \sigma_2 \leq \cdots \leq \sigma_N$, and further suppose that the $m$ most precise measurements are faulty; let the vector of the additive gross errors be $\boldsymbol{\epsilon}$ such that $\epsilon_i = 0$ for all $i > m$. By analyzing the least-squares adjustment equation as a projection, one can see that the impact of the faults $\boldsymbol{\epsilon}$ on the time estimate $\widehat{\delta t}$ is maximized when the fault vector $\boldsymbol{\epsilon}$ is collinear with $\boldsymbol{\Sigma}^{-1}\mathbf{1}$, where $\boldsymbol{\Sigma}$ is the diagonal matrix constructed from the measurement variances $\sigma_i^2$ and $\mathbf{1}$ is a vector of ones. This implies that the fault vector should have the following form:

$$\boldsymbol{\epsilon} = \begin{bmatrix} \sigma_1^{-2} / \sqrt{\sum_{i=1}^{m} \sigma_i^{-4}} \\ \vdots \\ \sigma_m^{-2} / \sqrt{\sum_{i=1}^{m} \sigma_i^{-4}} \\ 0 \\ \vdots \\ 0 \end{bmatrix} \|\boldsymbol{\epsilon}\|. \tag{4}$$

Consequently, the maximum timing error, $\tilde{t}_{MAX}$ due to a vector of faults with Euclidian norm $\|\boldsymbol{\epsilon}\|$ is obtained as

$$\tilde{t}_{MAX} = \frac{\sum_{i=1}^{m} \frac{\epsilon_i}{\sigma_i^2}}{c \sum_{i=1}^{N} \sigma_i^{-2}} = \frac{\|\boldsymbol{\epsilon}\|}{c} \frac{\sqrt{\sum_{i=1}^{m} \sigma_i^{-4}}}{\sum_{i=1}^{N} \sigma_i^{-2}}. \tag{5}$$

It remains to determine the value of $\|\boldsymbol{\epsilon}\|$ as a function of the known chi-square noncentrality parameter, $\delta$. Recall that $\delta$ corresponds to the sum of squares of the expected values of the residuals, which are no longer zero but composed of the error $\tilde{t}_{MAX}$ incurred in the weighted average estimate $\widehat{\delta t}$ and the measurement biases themselves:

$$\delta = \sum_{i=1}^{N} \mathrm{E}\left[\frac{\rho_i - r_i - c\,\widehat{\delta t}}{\sigma_i}\right]^2 = \sum_{i=1}^{m} \left( \frac{\frac{\|\epsilon\| \sigma_i^{-2}}{\sqrt{\sum_{j=1}^{m} \sigma_j^{-4}}} - \frac{\|\epsilon\| \sqrt{\sum_{j=1}^{m} \sigma_j^{-4}}}{\sum_{j=1}^{N} \sigma_j^{-2}}}{\sigma_i} \right)^2 + \sum_{i=m+1}^{N} \left( \frac{\frac{\|\epsilon\| \sqrt{\sum_{j=1}^{m} \sigma_j^{-4}}}{\sum_{j=1}^{N} \sigma_j^{-2}}}{\sigma_i} \right)^2. \tag{6}$$

Solving for $\|\boldsymbol{\epsilon}\|$ and substituting it to (5) gives the TPL:

$$TPL = \tilde{t}_{MAX} = \frac{1}{c \sum_{i=1}^{N} \sigma_i^{-2}} \sqrt{\frac{\delta \sum_{i=1}^{m} \sigma_i^{-4}}{\sum_{i=1}^{m} \left( \frac{\sigma_i^{-3}}{\sqrt{\sum_{j=1}^{m} \sigma_j^{-4}}} - \frac{\sqrt{\sum_{j=1}^{m} \sigma_j^{-4}}}{\sigma_i \sum_{j=1}^{N} \sigma_j^{-2}} \right)^2 + \sum_{i=m+1}^{N} \left( \frac{\sqrt{\sum_{j=1}^{m} \sigma_j^{-4}}}{\sigma_i \sum_{j=1}^{N} \sigma_j^{-2}} \right)^2}}. \tag{7}$$

It is noteworthy that the number of simultaneous faults $m$ is one of the input parameters for the computation of the TPL. As the value of $m$ is increased, the TPL degrades given that the other parameters are kept constant. Also note that the TPL, which is

derived from the global chi-square test (3), only quantifies the protection in terms of fault detection. In cases where fault exclusion is to be attempted, it is important that the weight of the biased measurements must be strictly less than 50 % in the time estimation; otherwise, the residuals of the intact observations become larger and cause the exclusion logic to fail. In contrast, when fault exclusion is not to be carried out, e.g., if only two satellites are available, this requirement is not necessary. However, in such cases, unbalanced measurement weighting degrades the TPL: intuitively, adding a measurement with a higher uncertainty does not contribute much to the time estimation, yet it has to be screened for outliers.

**Dual-Constellation Cross-Check**

If the receiver implements multi-constellation processing, the time information from another system can be used to cross-check the EGNSS based solution against undetected individual satellite faults or constellation-wide failures. Note that EGNOS receivers are inherently capable of this as they can compute a redundant GPS-only solution without applying the augmentation data; however, it should be noted that these two solutions are not entirely independent because they are based on the same tracking results.

Suppose that two clock bias solutions $\widehat{\delta t}_1$ and $\widehat{\delta t}_2$ were obtained with associated standard deviation estimates $\hat{\sigma}_1$ and $\hat{\sigma}_2$, respectively. The first task is to convert these two solutions to a common time scale either by applying the system-specific UTC offset parameters or an inter-system offset such as the GGTO. Again, in the absence of measurement faults, the errors in both solutions are assumed to follow zero-mean normal distributions with the respective standard deviations. Consequently, the difference of the two solutions follows a zero-mean normal distribution, which allows the cross-checking of their mutual consistency. Normalizing the difference of the two solutions by the expected standard deviation of the difference serves as test statistic, and the following test is conducted to assess if the zero-mean hypothesis holds:

$$|\hat{t}_1 - \hat{t}_2| < \mathrm{inv}N\left(1 - \frac{p_{FA}}{2}\right) \sqrt{\hat{\sigma}_1{}^2 + \hat{\sigma}_2{}^2 + \sigma_{CONV}^2 + \sigma_{CAL}^2}. \tag{8}$$

The variances $\sigma_{CONV}^2$ and $\sigma_{CAL}^2$ refer to the uncertainties in the time scale conversion parameters and the calibration of possible inter-system hardware biases, respectively; the function $\mathrm{inv}N(x)$ is the inverse cdf of the standard normal distribution. If the test criterion is satisfied, the solutions are declared as mutually consistent and the processing can be continued; otherwise, the solutions are rejected and holdover is triggered.

**Local Oscillator Steering and Holdover**

Once a consistent EGNSS timing solution is obtained, the last step is to verify it against the known stability properties of the LO before using it to generate steering corrections. For this purpose, we use the Kalman filter proposed in (Van Dierendonck et al. 1984) which uses the so-called $h_0$, $h_{-1}$, and $h_{-2}$ parameters to propagate the uncertainty in the time and frequency error estimates. These parameters characterize the white, flicker, and random walk frequency modulations, respectively, and can be determined based on the Allan deviation of the LO output (Riley 2008).

The state vector consists of the time and frequency offset estimates: $\boldsymbol{x} = [\delta t \quad \delta f]^T$. Note that only time offset measurement updates are being applied; the (normalized) frequency offset is estimated indirectly through the state transition model with the discrete-time transition matrix $\boldsymbol{\Phi}$ expressed as

$$\boldsymbol{\Phi} = \begin{bmatrix} 1 & T_s \\ 0 & 1 \end{bmatrix} \tag{9}$$

where $T_s$ denotes the update period (in units of seconds). The discrete-time process noise covariance $\boldsymbol{Q}$ is given by (Van Dierendonck et al. 1984)

$$\boldsymbol{Q} = \begin{bmatrix} \frac{h_0}{2} T_s + 2h_{-1}T_s^2 + \frac{2}{3}\pi^2 h_{-2}T_s^3 & 2h_{-1}T_s + \pi^2 h_{-2}T_s^2 \\ 2h_{-1}T_s + \pi^2 h_{-2}T_s^2 & \frac{h_0}{2T_s} + 2h_{-1} + \frac{8}{3}\pi^2 h_{-2}T_s \end{bmatrix}. \tag{10}$$

The EGNSS based time offset solutions $\widehat{\delta t}$ are used for the measurement updates in conjunction with their estimated standard deviations $\hat{\sigma}$. However, before actually applying the update, the measurement innovation is tested for outliers as

$$\left|\frac{\widehat{\delta t}-\boldsymbol{Hx}}{\sqrt{\boldsymbol{HPH}^T+\widehat{\sigma}^2}}\right| < \text{inv}N\left(1-\frac{p_{FA}}{2}\right) \quad (11)$$

where $\boldsymbol{P}$ is the estimated covariance matrix of the state vector $\boldsymbol{x}$ and the measurement matrix is given as $\boldsymbol{H} = [1 \quad 0]$. If the left-hand side exceeds the critical value, the newly obtained measurement is discarded as potentially faulty and no update is carried out. Such implausible measurements can be caused by, e.g., constellation-wide failures especially if the dual-constellation cross-check is not implemented.

## PRACTICAL EXAMPLES

In order to validate the robustness of the timing services against the identified threats, a range of tests have been specified. In this paper, we present a subset of them to analyze the effectiveness of the individual robustness concepts. All tests were conducted using a NovAtel ProPak6 receiver as the source of pseudorange measurements and navigation data which were processed using the FGI-GSRx software navigation engine. A low-cost temperature-compensated crystal oscillator (KVG Quartz Crystal Technology GmbH 2005) was used as the local oscillator, but no steering was implemented; this oscillator had a normalized frequency offset of $1.7 \times 10^{-7}$. UTC(MIKE) was used as the reference time. For a more detailed description on the testing methodology for timing receivers, refer to, e.g., (Ogrizović et al. 2013; Kirkko-Jaakkola et al. 2017).

### Interference Detection

To illustrate the AGC-based interference detection, consider a meaconing scenario. The test configuration is a Galileo E1–E5 receiver with both frequencies being spoofed simultaneously by a signal repeater. The power of the spoofing signal is increased in a stepwise manner according to Table 1. The entire experiment spanned 2200 seconds.

**Table 1 Meaconing signal strength**

| Time (s) | Spoofing/signal ratio (dB) |
|---|---|
| 420 | –20 |
| 840 | –10 |
| 1140 | 0 |
| 1440 | +10 |

The resulting timing error experienced by the receiver without any mitigation is shown in Figure 4; the blue line shows the timing solution before the LO steering and without Kalman filtering. The green line shows the impact of the Kalman filter. It can be seen that initially, the spoofing signal has a similar effect as multipath: the two curves in Figure 4 experience an increasing error up to a maximum of about –60 ns. At this point, the power of the repeater is so high that the receiver no longer tracks a combination of the useful and spoofed signal. A sudden jump is observed indicating that after about 1200 seconds only the spoofed signal is tracked. In this case, the Kalman filter alone does not provide any additional benefit. In particular, the KF-based outlier testing is not efficient against this attack because of its gradual nature. The AGC gains for E1 and E5 radio frontends are shown below the timing results; the gain decreases visibly as the spoofing power increases, suggesting that the AGC can point out the presence of not only jammers but even spoofing signals

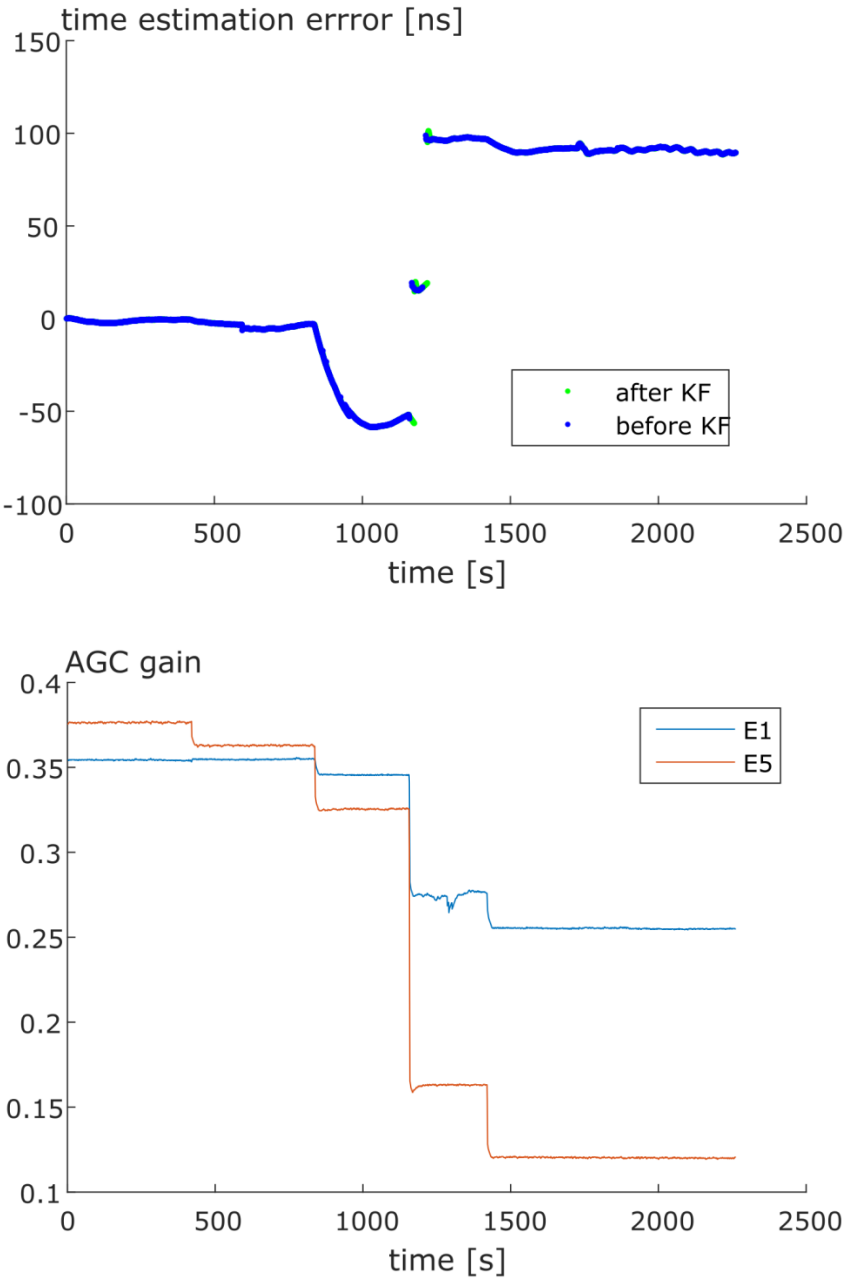


**Figure 4: Timing solution (top) and AGC gain (bottom) for a receiver under meaconing.**

**Individual Satellite Failure**

Let us examine the role of T-RAIM on the envisioned timing services. In this scenario, an EGNOS receiver is subject to a gross measurement error, e.g., tracking a reflected non-line of sight signal where the augmentation data have no direct effect. The result can be seen in the top plot of Figure 5 where the fault starts after one hour and is present for seven hours. It is acknowledged that a long-time constant bias error due to a signal reflection is not a realistic scenario as such, but it serves for illustrative purposes.

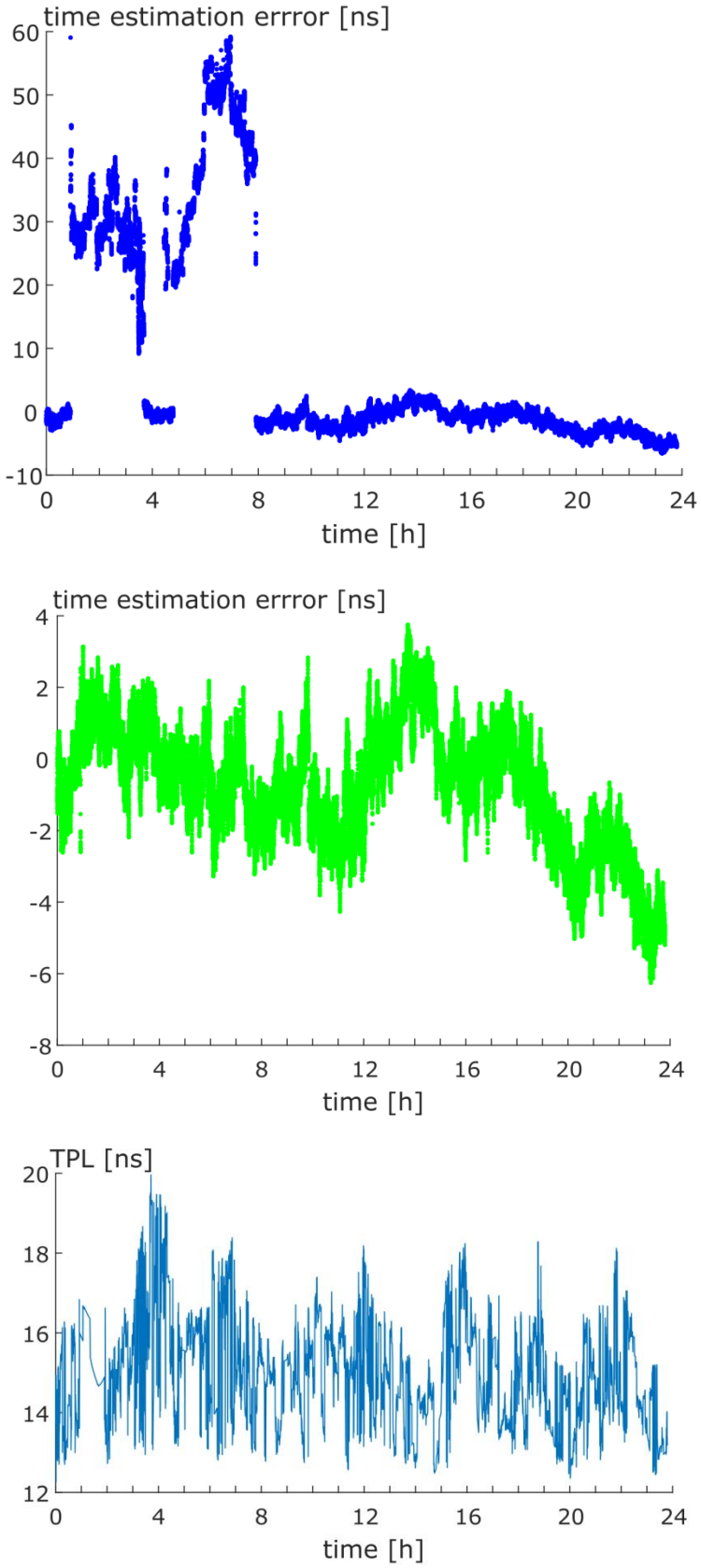


**Figure 5: Effect of T-RAIM. Top: time offset solution without mitigation; middle: time offset with T-RAIM excluding the outlier; bottom: TPL determined with $p_{FA} = 10^{-5}$ and $p_{MD} = 10^{-3}$.**

The middle plot of Figure 5 shows the resulting timing errors after applying T-RAIM; it can be seen that the outlier has been successfully detected and excluded. The bottom subfigure shows the corresponding TPL, which does not exceed 20 ns during the experiment. It can be seen that for most of the time, the obtained TPL values are stricter than the timing errors seen without T-RAIM which implies that T-RAIM should be able to detect them subject to the chosen missed detection threshold, as was the case. Moreover, the TPL values clearly bound the time estimation errors after excluding the fault, which are in the order of 5 ns. When computing the TPL, the maximum number of simultaneous faults $m$ was given the maximum possible value at each epoch, i.e., the size of the largest satellite subset that cannot exceed 50 % of the total measurement weight; accounting for a smaller number of outliers only would have resulted in stricter TPL values.

**Dual-Constellation Cross-Check**

In this test we consider the scenario where a false solution has passed the T-RAIM consistency test for one constellation. The starting point is illustrated in the top plot of Figure 6 where, in this case, the Galileo timing solution is severely corrupted for a certain period. Simultaneously, the solution obtained using GPS is intact (not shown in the figure).

The middle subplot of Figure 6 shows the detection statistic for the dual-constellation cross-check. It can be seen that the time offset detection threshold, which has been computed with $p_{FA} = 10^{-5}$, corresponds approximately to 100 ns. Depending on the requirements of the particular timing application, it may be necessary to increase the false alarm rate to obtain a stricter threshold. The error in the Galileo solution exceeds this limit clearly and the inconsistency can be detected. Applying holdover during the period of inconsistency results in the timing error shown in the bottom plot of Figure 6. Note that the holdover period spans approximately 3 hours. It can be seen that the maximum wander in the time offset during that period is roughly 700 ns, which is several orders of magnitude better than the 50 μs error experience when holdover is not triggered. This effect is illustrated in the upper plot of Figure 6. The behavior during holdover is dependent on the choice of LO; for instance, a more stable oven-controlled crystal oscillator could sustain longer holdover times than the low-cost clock (KVG Quartz Crystal Technology GmbH 2005) used in these experiments.

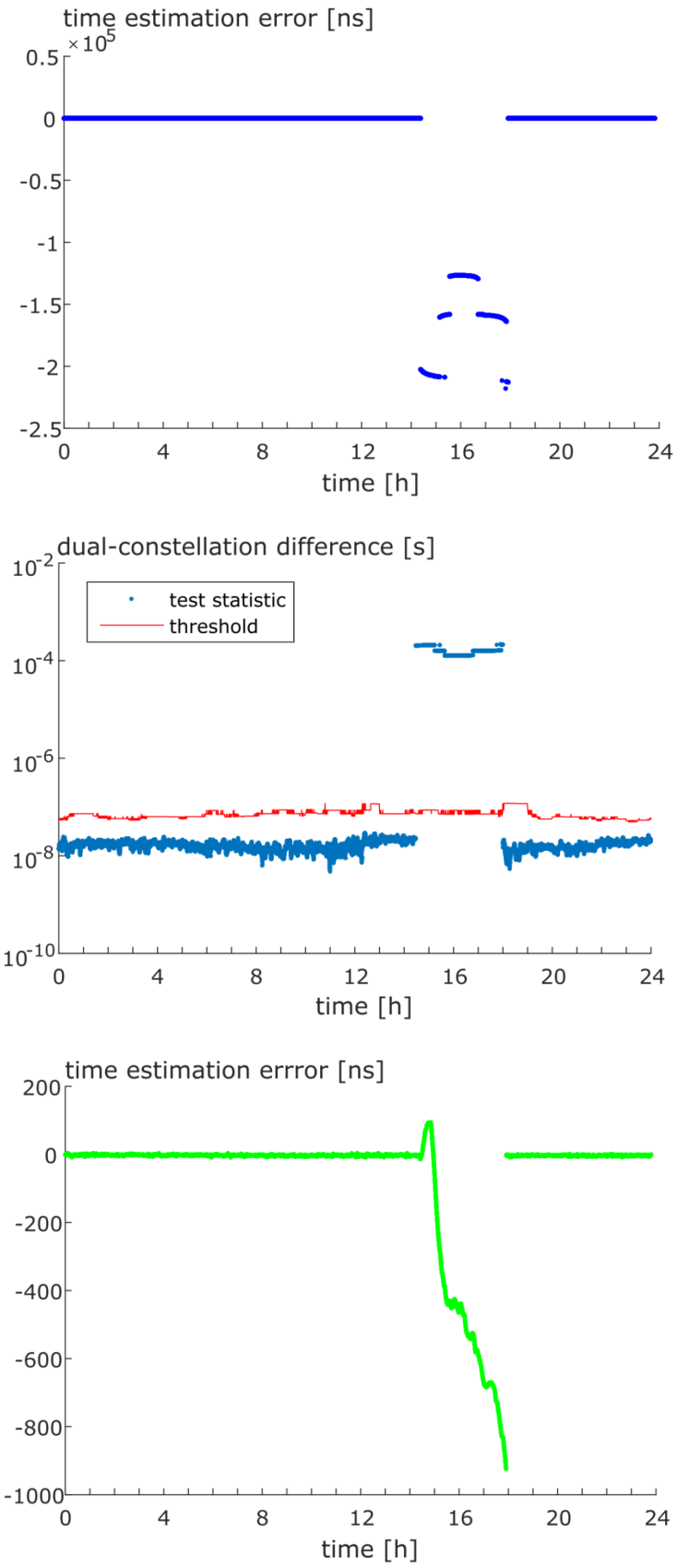


**Figure 6: Application of the dual-constellation cross-check. Top: Galileo timing solution temporarily corrupted when no mitigation is applied; middle: detection statistic from (8); bottom: timing solution mitigated by holdover.**

## CONCLUSIONS

This paper presented a set of technical options to enhance the robustness of EGNSS timing receivers, with the ultimate goal of specifying stand-alone EGNSS timing services. These options include algorithms that are applied at various stages of the receiver-side processing. Combining these methods together makes it possible to address the most relevant threat scenarios that can compromise the integrity of EGNSS based timing, including threats caused by single satellite failures, constellation-wide faults, and local effects such as radio frequency interference or spoofing.

The test results confirmed the capability of excluding individual measurement outliers to recover a consistent EGNSS timing solution as well as to detect misleading information by means of interference detection and verification with another GNSS constellation or through the LO itself. If the timing solution is regarded as unreliable, it is discarded and the LO continues operation in holdover mode; therefore, a sufficiently stable LO must be used to fulfil the requirements of the particular timing application.

## ACKNOWLEDGMENTS

This research has been conducted within the project "Advanced Mission Concepts: R&D for Robust EGNSS Timing Services" funded by the Directorate-General for Internal Market, Industry, Entrepreneurship and SMEs (DG-GROW) of the European Commission.

## REFERENCES

F. Bastide, D. Akos, C. Macabiau, and B. Roturier (2003), "Automatic gain control (AGC) as an interference assessment tool," in Proc. ION GPS, Portland, OR, pp. 2042–2053.

A. Bauch and P. Whibberley (2017), "Reliable Time from GNSS Signals," Inside GNSS, 12(2), pp. 38–44.

J. Blanch, T. Walter, P. Enge, S. Wallner, F. Amarillo Fernandez, R. Dellago, R. Ioannides, I. Hernandez Fernandez, B. Belabbas, A. Spletter, and M. Rippl (2013), "Critical Elements for a Multi-Constellation Advanced RAIM", NAVIGATION, Journal of The Institute of Navigation, 60(1), pp. 53–69.

D. Borio, F. Dovis, H. Kuusniemi, and L. Lo Presti (2016), "Impact and Detection of GNSS Jammers on Consumer Grade Satellite Navigation Receivers," Proceedings of the IEEE, 104(6), pp. 1233–1245.

P. Defraigne, N. Guyennon, and C. Bruyninx (2008), "GPS time and frequency transfer: PPP and phase-only analysis," International Journal of Navigation and Observation, doi: 10.1155/2008/175468

European GNSS Agency (2015), "EGNOS Open Service (OS) Service Definition Document," issue 2.2. ISBN 978-92-9206-018-3, doi:10.2878/204958

European Commission (2016a), "Galileo Initial Services – Open Service – Service Definition Document," issue 1.0.

European Commission (2016b), "European GNSS (Galileo) Open Service – Ionospheric Correction Algorithm for Galileo Single Frequency Users," issue 1.2.

G. J. Geier, T. M. King, H. L. Kennedy, R. D. Thomas, and B. R. McNamara (1995), "Prediction of the time accuracy and integrity of GPS timing." In Proc. 49th Frequency Control Symposium, San Francisco, CA, pp. 266–274.

C. Hegarty, E. Powers, and B. Fonville (2004), "Accounting for timing biases between GPS, modernized GPS, and Galileo signals." In Proc. Precise Time and Time Interval Meeting, Washington, D.C., pp. 307–317.

M. Kirkko-Jaakkola, S. Thombre, S. Honkala, S. Söderholm, S. Kaasalainen, H. Kuusniemi, H. Zelle, H. Veerman, and A. Wallin (2017), "Evaluating the Robustness of EGNSS Based Timing Services," in Proc. European Navigation Conference, Lausanne, Switzerland.

H. Kuusniemi (2005), "User level reliability and quality monitoring in satellite based personal navigation." Doctoral Dissertation, Tampere University of Technology, Tampere, Finland.

KVG Quartz Crystal Technology GmbH (2005), "T-9601F data sheet.", Neckarbischofsheim, Germany.

M. A. Lombardi (2006), "Legal and Technical Measurement Requirements for Time and Frequency," Measure 1(3), pp. 60–69.

A. Mujunen, J. Aatrokoski, M. Tornikoski, and J. Tammi (2016), "GPS Time Disruptions on 26-Jan-2016." Aalto University publication series Science + Technology 2/2016, Helsinki, Finland.

V. Ogrizović, J. Marendić, S. Renovica, S. Delčev, and J. Gučević (2013), "Testing GPS generated PPS against a rubidium standard," Acta IMEKO 2(1).

W. J. Riley (2008), "Handbook of Frequency Stability Analysis." NIST Special Publication 1065, National Institute of Standards and Technology, Boulder, CO.

A. J. Van Dierendonck, J. B. McGraw, and R. G. Brown (1984), "Relationship between Allan variances and Kalman filter parameters." In Proc. Precise Time and Time Interval Applications and Planning Meeting, Greenbelt, MD, pp. 273–293.

Paper first presented at the ION GNSS+ conference, Portland, Oregon, September 2017.